AGU PUBLICATIONS

Space Weather

RESEARCH ARTICLE
10.1002/2013SW001007

Key Points:
- Manuscript assesses current and near-future space weather assets
- Current assets unreliable for forecasting of severe geomagnetic storms
- Near-future assets will not improve the situation

Supporting Information:
- STEREO downlink (text)
- STEREO downlink

Correspondence to:
A. Posner,
arik.posner@nasa.gov

Citation:
Posner, A., M. Hesse, and O. C. St. Cyr (2014), The main pillar: Assessment of space weather observational asset performance supporting nowcasting, forecasting, and research to operations, *Space Weather*, *12*, 257–276, doi:10.1002/2013SW001007.

Received 29 OCT 2013
Accepted 19 MAR 2014
Accepted article online 23 MAR 2014
Published online 15 APR 2014

The main pillar: Assessment of space weather observational asset performance supporting nowcasting, forecasting, and research to operations

A. Posner[1,2], M. Hesse[1], and O. C. St. Cyr[1]

[1]NASA Goddard Space Flight Center, Greenbelt, Maryland, USA, [2]Also at NASA Headquarters, Washington, DC, USA

Abstract Space weather forecasting critically depends upon availability of timely and reliable observational data. It is therefore particularly important to understand how existing and newly planned observational assets perform during periods of severe space weather. Extreme space weather creates challenging conditions under which instrumentation and spacecraft may be impeded or in which parameters reach values that are outside the nominal observational range. This paper analyzes existing and upcoming observational capabilities for forecasting, and discusses how the findings may impact space weather research and its transition to operations. A single limitation to the assessment is lack of information provided to us on radiation monitor performance, which caused us not to fully assess (i.e., not assess short term) radiation storm forecasting. The assessment finds that at least two widely spaced coronagraphs including L4 would provide reliability for Earth-bound CMEs. Furthermore, all magnetic field measurements assessed fully meet requirements. However, with current or even with near term new assets in place, in the worst-case scenario there could be a near-complete lack of key near-real-time solar wind plasma data of severe disturbances heading toward and impacting Earth's magnetosphere. Models that attempt to simulate the effects of these disturbances in near real time or with archival data require solar wind plasma observations as input. Moreover, the study finds that near-future observational assets will be less capable of advancing the understanding of extreme geomagnetic disturbances at Earth, which might make the resulting space weather models unsuitable for transition to operations.

1. Introduction

This manuscript discusses an assessment concerning to what extent space hardware, i.e., the combinations of sensors and spacecraft exposed to the changing conditions in space, can reliably provide near-real-time (NRT) information for space weather forecasting, by taking into account the underlying mission and data pipeline architecture. Also, an important consideration is whether sufficient observational information can be preserved and recovered after the storm in order to improve modeling capabilities of extreme events. A particular focus of this study is the capability of forecasting extreme space weather events that are caused by Earth-directed coronal mass ejections (CMEs). We adapt the definition of extreme space weather events from *Riley* [2012] as "something we have not experienced in the space era … which could result in significant adverse consequences." Our single strict assessment criterion is reliability (and availability) of critical space weather observations during such historically extreme storms by the key examples provided to us of less severe storms.

The present analysis is a snapshot in time in the sense that any addition or removal/loss of assets could alter the outcome. The assessment is done at a moment when short- and long-term geomagnetic storm, ionospheric disturbance, and geomagnetically induced current (GIC) forecasting caused by interplanetary CMEs foremost depend on observations provided by NASA and NASA-supported teams. Other relevant space weather phenomena, such as solar energetic particle occurrence leading to radiation storm conditions at 1 AU, could also be assessed in this way. In order to do so, a complete picture could only be achieved with information on particle detector performance from other agencies that is not available to the authors at this time.

Hazards of severe solar activity derive from energetic processes close to the Sun that can lead to sudden increases in the fluxes of highly energetic ions near Earth and from intense X-ray and radio emissions from the Sun's direction.

High-speed clouds of plasma carry magnetic fields from the Sun to 1 AU that upon impact can interact with and dramatically change Earth's magnetic field. These changes can induce strong currents into long wires, once telegraph lines and now predominantly power lines. These GICs can affect or even completely disable power grids on various scales, and studies [*Kappenman*, 2005; *National Research Council Workshop of the National Academies,* 2009; *Zurbuchen*, 2012] show that the potential economic impact in the US can be enormous. Space weather effects pose a formidable challenge to engineering storm-proof technological systems and to research in order to reliably forecast effects in a way that protective measures can be taken in time.

The question of how large the extrema of space weather can become is currently under debate. For example, a historically significant space weather event occurred on 1 September 1859. Richard Carrington witnessed a rare white-light flare while observing the Sun with a solar telescope. Eyewitness accounts of aurorae at low magnetic latitudes, and magnetometer records suggest a very fast, $<$17 h [*Carrington*, 1859; *Cliver and Svalgaard*, 2004] propagation time of the CME from Sun to Earth as compared to the more typical solar wind propagation time of ~72 h. Early ground-based magnetometer readings have been interpreted as equivalent to the disturbance storm time (*Dst*) index value of -850 to $-1{,}760$ [*Siscoe et al.*, 2006; *Tsurutani et al.*, 2003], which, although contamination by auroral currents may be possible, would so far be unsurpassed in the space age. As a context, geomagnetic storm conditions are considered severe when *Dst* dips below -150. *Riley* [2012] statistically analyzed occurrence rates of space weather parameters including *Dst* and predicted that the likelihood of occurrence during the next decade of a similar or larger storm would be ~12%.

Quantitative space-based measurements of space weather events became available a century later. Significant recent outbursts of solar activity occurred in late October/early November of 2003. These Halloween storms unleashed a series of X-class flares, among them record-breaking flares with magnitudes X17 and X28 [*Oler*, 2004] and fast CMEs. Two of the Earth-directed CMEs impacted the magnetosphere directly, while reaching record speed levels at or beyond 1900 km/s, surpassing the previous space-age record-holding August 1972 storm of 1700–1800km/s [*Skoug et al.*, 2004; *Farrugia et al.,* 2005]. For context, lists of known fast-transit events can be found in *Cliver and Svalgaard* [2004] and *Cliver et al.* [1990]. The Halloween storms caused *Dst* readings of -353 and -371 in two consecutive surges within a 24 h period (followed later by another burst of activity with *Dst* reaching -422 on 20 November 2003 the following solar rotation). Published reports on the impacts of these events include scientific studies of the events [e.g., *Lopez et al.*, 2004; *Skoug et al.*, 2004; *Zurbuchen et al.*, 2004], damage assessments [e.g., *Kappenman*, 2005; *Pulkkinen et al.*, 2005], and evaluations of forecasting performance [e.g., *Barbieri and Mahmot*, 2004; *Dryer et al.*, 2004; *Evans et al.*, 2004; *Oler*, 2004].

This manuscript focuses specifically on the performance of the sum of the NASA space-based instrument hardware, including those providing NRT observations required for input in forecasting tools and models, an aspect that previously has not been looked at systematically. In section 2, we lay out the definitions, criteria, and the methodology of the space weather assessment. In section 3, we apply the methodology and criteria to the collected data. Section 4 discusses the overall assessment result.

2. SWx Assessment Methodology: Space Weather Types, Scales, and Assessment Criteria

2.1. General Methodology

Our methodology is guided by the potential harm of extreme events that was discussed in a study published by the *National Research Council Workshop of the National Academies* [2009], which is significantly above the potential harm caused by moderate space weather. Our single strict assessment criterion is reliability (and availability) of critical space weather observations during historically extreme storms. This assessment criterion is now supported by a survey of space weather users [*Schrijver and Rabenal,* 2013] that finds that many private sector and government users request better "location-specific or sector-specific forecasts" that can only be obtained with geospace models running in near real time. The methodology of this study is to collect performance data of space weather assets and match them against sets of requirements that derive directly from our assessment criterion. The performance data to be analyzed are twofold: (1) NRT assessment: Would the collected data meet the needs for NRT use of space weather models in order for them to reflect up-to-date geospace conditions that could be used for advance warning of inclement space weather

conditions? (2) Archival assessment: Would data obtained during extreme space weather be of the quality needed in order to be used as input into space weather models in order for researchers to meaningfully assess and improve model performance?

A key role in this assessment is played by the current status of understanding space weather through forecasting models. It is recognized that specific space weather phenomena have certain sets of input data requirements to be met and certain lead times associated with them.

Section 2.2 describes the specific space weather time scales that are important for the NRT assessment. Section 2.3 describes various current methods of forecasting space weather effects and their data requirements. Subsection 2.4 summarizes all data requirements.

2.2. Space Weather Time Scales

For the NRT assessment, it is important to define the available lead times for space weather forecasting based on event precursor observations.

2.2.1. Definition of No Lead Time

Some space weather phenomena, those propagating at the speed of light, cannot be forecasted in NRT based on precursor observations of the event itself; i.e., their lead time is zero. These phenomena include solar flaring in X-rays and EUV, and radio bursts. Their effects include ionospheric disturbances that influence radio communications or spacecraft drag, direct interference with radio communications, and direct spacecraft charging/discharging.

2.2.2. Short Lead-Time Definition

As described in section 1, significant geomagnetic storms are the direct consequence of (interplanetary) coronal mass ejections (ICMEs) propagating from the Sun to the Earth. Key space weather data are obtained about 1.5 million km upstream of Earth near the Lagrangian Point 1 (L1), where the gravitational pull of Sun and Earth-Moon balance [*Farquhar*, 1970]. Since the days of the International Sun-Earth Explorer (ISEE) 3 [*Ogilvie et al.*, 1978; *Dunhak*, 1979], this is assumed a standard location for in situ space weather measurements, as large-scale solar wind plasma and magnetic field structures passing by L1 will eventually encounter Earth's magnetosphere. The important parameters that are needed in order to forecast processes in the Earth's magnetosphere and ionosphere are solar wind plasma velocity, density, temperature, and magnetic field vector, ideally from the location directly upstream of the Earth. We take into account the radial distance of L1 from the Earth's magnetosphere (~1,440,000 km) in connection with the range of radial speeds of transient disturbances at L1 for geomagnetic storm warnings in NRT from assets at L1. The potential available warning time is on the order of 10–12 min for (historic) extreme space weather events but extends to ~1 h for typical solar wind conditions (which, however, rarely lead to significant space weather events).

2.2.3. Definition of Long Lead Time

Another method of obtaining key space weather data is to observe the Sun remotely, so the available warning time is determined by the propagation time of a transient disturbance from the Sun to 1 AU. This potential available warning time is on the order of 15 h for (historic) extreme space weather events but extends to ~3 days for typical space weather conditions. Indeed, in July 2012, a CME transited the distance Sun-Earth orbit in about 17 h, as measured by NASA's STEREO-A spacecraft.

Note that long lead-time (LLT) forecasting is not restricted to remote-sensing observations through electromagnetic radiation, as warning methods have been devised that include in situ observations as precursors of the transient disturbances, e.g., cosmic ray protons or suprathermal protons. The long-term forecasting methods can include as input coronagraph observations from the Sun-Earth line (including L1) or coronagraph and heliospheric imager observations that cover the Sun-Earth line. Also useful for long-term forecasting are EUV, X-ray, and/or H-alpha images of the Sun from on or off the Sun-Earth line but ideally from locations near quadrature with Earth. All these observations aid in determining the initial direction, speed, and longitudinal extent of the CME. Solar radio observations that cover type-II radio bursts also give indirect information on the propagation of CMEs by measuring the signal of particle acceleration of CME-driven shocks near the Sun and as they transit the inner solar system. The heliospheric imager method, looking at CME propagation along the Sun-Earth line, actually bridges the gap between long- and short-term forecasting methods, and so do other parameters measured in situ. These include suprathermal ions that constantly stream away along interplanetary magnetic field lines from the CME-driven shock front. Cosmic rays that propagate along the interplanetary magnetic field lines also provide information on approaching

arrivals of magnetic field compressions or magnetic clouds associated with interplanetary CMEs [*Munakata et al.*, 2000].

2.2.4. Definition of Extended Lead Time

It is recognized that fast solar wind streams of corotating interaction regions (CIRs) have geomagnetic effectiveness [*Tsurutani et al.*, 1995] and that their arrival can be forecasted with several methods. One method extrapolates observations from any location trailing Earth in its orbit by assuming quasi-stationary solar wind structure. Such structure would quasi-rotate with the synodic angular rotation rate of the Sun and eventually catch up with Earth. The potential warning time of the extended lead-time (ELT) method is on the order of 1 week from the quadrature position but depends on the actual angular separation between the trailing spacecraft and Earth and any necessary correction for radial distance from the Sun [*Simunac et al.*, 2009].

2.2.5. Definition of Lead Time Based on Preevent Observations

This time scale, still to be defined, would likely derive from probabilistic forecasting of solar activity or from helioseismic methods. Forecasting events before they occur at the Sun would be the only way to warn against effects from (light speed) solar radio and X-ray emission.

2.3. Space Weather Forecasting Models and Data Requirements

2.3.1. No Lead-Time Forecasting Models and Data Requirements

The space weather phenomena falling under this category can only be observed in NRT, which could include providing "nowcasting" information, but by definition they cannot be forecasted. Thus, there are no data requirements for forecasting.

2.3.2. Short Lead-Time Forecasting Models and Data Requirements

Most experimental models of the Sun-Earth system and in particular of the geospace system require reliable solar wind data as input and therefore fall under the short lead-time (SLT) category. Models that are driven by solar wind data include, e.g., forecasting of the arrival and effects of CIRs at Earth [*Williams et al.*, 2011; *Riley et al.*, 2010]; *Kp* and *Dst* forecasting [*Newell et al.*, 2007; *Tóth et al.*, 2007; *Horton and Doxas*, 1998; *Spencer et al.*, 2007]; magnetopause standoff distance and magnetic field forecasting at geostationary orbits [*Tóth et al.*, 2007]; radiation belt and ring current parameter forecasting [*Zheng et al.*, 2003; *Weigel et al.*, 2003]; GIC, Joule heating, and polar cap magnetic potential forecasting [*Tóth et al.*, 2007]; and quantitative forecasting of ionospheric response including composition, density, and temperature, and high-frequency communications conditions [*Fuller-Rowell et al.*, 2000; *Codrescu et al.*, 2012; *Manoj and Maus*, 2012; *Eccles et al.*, 2005]. Most of these models have versions implemented that undergo testing in NRT, e.g., at the NASA integrated Space Weather Analysis system (iSWA, http://iswa.gsfc.nasa.gov) [*Maddox et al.*, 2010]. Furthermore, many of these models undergo verification and validation with archival data, in particular for evaluating their performance at the Community-Coordinated Modeling Center (CCMC, http://ccmc.gsfc.nasa.gov), e.g., through Geospace Environment Modeling (GEM) challenges [*Pulkkinen et al.,* 2011; *Rastaetter et al.,* 2011; *Rastaetter et al.,* 2013], and in the transition of such models to potential operational use [*Pulkkinen et al.,* 2013]. A temporary loss of fidelity of solar wind input stream, e.g., for the period of 30 min or more, would render useless one third of all NRT products currently supported by iSWA, and if data is not recoverable, the same would apply to archival model testing.

The transfer of energy and momentum between the solar wind and Earth's magnetosphere takes place at the Earth's magnetopause through compression and magnetic reconnection and generates storms and substorms in the magnetosphere [*Arnoldy*, 1971; *Gonzalez et al.*, 2002]. For this purpose, accurate information on the variable interplanetary magnetic field (IMF) from upstream Earth is required but, by itself, not sufficient for forecasting the Earth's magnetospheric response.

There have been several studies linking L1 solar wind observations with locations near Earth that are relevant for the discussion of observational requirements. The achievable accuracy of this method has been analyzed by *Richardson et al.* [1998] with ISEE3. While plasma correlations between L1 and Earth are on average ~0.6, in particular the large changes in density that are associated with major disturbances are highly correlated, with r being ~0.85. *Petrukovich et al.* [2001] looked at this problem from a different angle, the energy input into the magnetosphere as derived by solar wind at Wind (between 30 Re and L1) and Interball (near Earth, $<$25 Re) observations. They found that differences between far-upstream and near-Earth inputs are of decreasing consequence with increasing storm strength. More recent studies [*Weimer et al.*, 2002, 2003]

found that tilted IMF fronts are the cause for apparent propagation delays between IMF structures near L1 and the magnetosphere. Multiple-variance analysis techniques for single spacecraft can be used to identify the IMF front tilt angle and correct for the delays, but they require between 7 and 30 min of IMF observations, which would add significantly to latency. On the other hand, *Richardson et al.* [1998] determined that solar wind plasma fronts have on average half the inclination of IMF fronts, which mitigates this effect on timing for solar wind plasma parameters. In fact, these measurements should ideally be taken over some spatial range in order to account for spatial variations of arriving solar wind and IMF fronts, as also suggested in *Weimer et al.* [2003]. Note also that the above findings have been reached by analyzing common solar wind conditions. It is therefore unknown how accurately, under extreme conditions, L1 solar wind plasma and magnetic field parameters would reflect those at the subsolar magnetopause if propagated along the GSE X direction, but indications are [*Richardson et al.*, 1998] that such differences play less and less a role with increasing storm strength.

The technique of short-term forecasting of the arrival of transient geomagnetic storms at Earth and for the prediction of their specific impacts requires a combination of solar wind plasma and magnetic field measurements, but their relative importance needs to be discussed. *Newell et al.* [2007] and *Pulkkinen et al.* [2010] discuss the evolution over time of the usage of coupling functions, i.e., the combination of solar wind parameters thought to be driving the magnetosphere and the ionosphere.

Accuracy and relative importance need to be taken into account when discussing observational requirements. Accuracy on the order of ~5% in the range of 250–2500 km/s would result in an arrival time accuracy of 5 min with slowest solar wind assuming solar wind fronts perpendicular to GSE X (down to ~3 min at 400 km/s). At all speeds, however, presumably the accuracy requirements of models would be driven by the need to quantify the energy transfer from the solar wind to the magnetosphere, e.g., affecting the magnetopause standoff distance. Although a linear relationship for energy transfer from the solar wind in to the magnetosphere via electromagnetic coupling exists [e.g., *Gao et al.,* 2012], the compression effects of the magnetosphere are related to kinetic coupling, which is proportional to v^2 (i.e., ~10% inaccuracy) and which also suggests that 5% accuracy in the solar wind velocity, might not be sufficient for high-precision forecasts. It should be mentioned again that a (single) one-dimensional measurement of the solar wind does not constrain the three-dimensional character of a shock front. A complete lack of knowledge, however, of either the solar wind density and speed or the magnetic field parameter would render accurate forecasts impossible [*Claudepierre et al.,* 2010] and further render most complex models useless for operational applications.

Magnetosphere and ionosphere models, both undergoing testing in NRT and with archival data, require certain time resolution of solar wind measurements. For example, runs of the *Weimer* [2005] ionospheric electrodynamical model require input time resolution of 1/min or better. Furthermore, applications of the Space Weather Modeling Framework [*Tóth et al.*, 2007] combined with GIC forecasting models require similar or better (10/s) time resolution. Since determination of GICs requires, as a key ingredient, the fluctuation level of ionospheric currents, it is conceivable that even higher time resolutions may be required in the future, when models mature further. For the NRT assessment, such observations would require at a minimum that the time resolution be better than the difference of propagation time and latency (~2 min), i.e., ~10 min.

2.3.3. Long Lead-Time Forecasting Models and Data Requirements

Several models are in existence that do not require solar wind observations as input but instead simulate disturbance propagation from the Sun to and beyond 1 AU (again *Tóth et al.* [2007] but also *Odstrčil and Pizzo* [1999] and *Arge and Pizzo* [2000]). Inputs into these models include solar remote sensing, including solar magnetograph observations, EUV, and X-ray imaging, and analysis of CME coronagraph observations. Although largely successful in reproducing hydrodynamic solar wind features at 1 AU, these models are hampered by our current lack of understanding of solar wind acceleration and CME initiation [e.g., *Tóth et al.*, 2007], in particular in their attempts to reproduce the fine structure of the solar wind magnetic field and of the magnetic structures embedded in CMEs that are so critical for geospace modeling. It is therefore widely accepted that until sufficient understanding is reached, solar wind observations from L1 would be needed in order to properly understand, simulate, and forecast space weather activity in geospace.

Current, conventional long-term forecasting of geomagnetic storms is based on observations made during and after the solar event occurs. For this, remote sensing of CMEs near the Sun [*Hudson et al.*, 2006] can be utilized in order to predict the direction and possible arrival of the disturbance at 1 AU. A particular focus is on

those CMEs propagating along the Sun-Earth line. From the Earth's point of view, these halo CMEs generate faint coronal signatures all around the Sun that can be exploited for forecasting. LASCO [*Brueckner et al.*, 1995] on SOHO has provided observations from L1 on the Sun-Earth line [e.g., *Howard et al.*, 1982; *St. Cyr et al.*, 2000].

As halo CMEs are at times hard to identify due to their rather faint signals, observations from multiple vantage points around the Sun make it easier to directly identify the event, its size, and its direction. The speed of the CME can also be determined with better accuracy when, from the point of view of the observational asset, the nose of the CME is in or near the plane of the sky. In order to determine its propagation direction, solar disk information in EUV or X-rays is useful, although it is considered more accurate to determine its propagation direction with multiple coronagraphs widely distributed in space. Such observations currently are provided by Sun Earth Connection Coronal and Heliospheric Investigation (SECCHI) [*Howard et al.*, 2008] onboard the two STEREO spacecraft. In early 2011, they passed the quadrature mark of 90° angular distance from Earth, adding approximately 22° per year in elongation.

The most advanced model currently in use with NRT data, WSA-ENLIL [*Odstrčil and Pizzo*, 1999; *Odstrčil et al.*, 2004; *Xie et al.*, 2004], incorporates into a background solar wind the propagation direction, latitudinal angular extent, and propagation speed of a cone of plasma. Its launch time, direction, extent, and speed are modeled based on CMEs observed by STEREO and SOHO coronagraphs. Simulations provide advance knowledge of encounters of the simulated CME front with Earth's magnetosphere but also for other assets in the inner heliosphere including in planetary orbits.

Imaging of CME onsets is also possible by EUV observations of the solar disk and limb regions with the high cadence and resolution provided by the Solar Dynamics Observatory (SDO). However, these auxiliary observations would need to be incorporated into models before an assessment on the utility of the data source can be made. The available advance warning time matches that of the coronagraph method.

There exists an independent method of long-term geomagnetic storm forecasting that utilizes shock signatures ahead of fast CMEs in the corona. Type-II radio bursts are an indirect sign of electron acceleration at the shock front that can be observed from space, and their procession in frequency provides an indication of shock propagation speed. The performance of models for geomagnetic storm forecasting based on type-II and X-ray observations has been analyzed by *Fry et al.* [2003] and provides the same warning time potential as the coronagraph method. A shock-arrival forecasting technique relying on space-based observations of low-frequency type-II events has been described by *Cremades et al.* [2007]. Not all CME/shocks produce radio noise, so all of these techniques are limited in their forecasting ability.

Approaches of magnetic clouds can be detected in advance through their effects on the cosmic ray flux [*Munakata et al.*, 2000]. An approaching CME deflects cosmic rays coming from the sunward direction, reducing the cosmic rays flux that would otherwise reach the observer (e.g., Earth or L1). The decrease in cosmic ray flux due to the loss cone, a narrow region of pitch angles around the sunward IMF direction, can be detected on the order of 6 h in advance, with reports of up to 1 day in advance.

The presence of keV ion foreshocks populating an extended region ahead of a fast CME and usually peaking at shock passage (energetic storm particles, ESPs) can be utilized as an advance warning signal if observations of suprathermal particle detectors are available [see, e.g., *Smith and Zwickl*, 1999; *Lario et al.*, 2003, and *Posner et al.*, 2004]. The potential advance warning time ranges from hours up to a day.

One commonality of long-term geomagnetic storm forecasting models, with the notable exception of the cosmic ray decrease method, is the lack of any information they provide on geoeffectiveness of the potential magnetic structure embedded in the disturbance behind the shock front. However, although the cosmic ray decrease method may signal in advance the presence of a magnetic cloud, it does not provide the crucial information on its internal structure.

The advantage of these methods is that longer lead times on the order of 0.25 to 3 days can be achieved, as compared to the short-term forecasting method discussed above. On the other hand, the precision of these methods is much lower than that of the short-term forecasting method. Despite improvements in forecasting accuracy over the years, led by the remote sensing of CMEs, the error bars remain at approximately 7.5 to 10 h [*Millward et al.*, 2013; *Falkenberg et al.*, 2011; *Gopalswamy et al.*, 2001]. Performance issues and positions of the sensors, as discussed in the following section, could affect this accuracy.

Table 1. Summary of Requirements for the Main Forecasting Methods, Short- and Long-Lead Time Geomagnetic Storm Forecasting[a]

Space Obs. Requirement	SLT Geomagnetic Storm Forecasting	LLT Geomagnetic Storm Forecasting	ELT CIR Arrival Time Forecasting[a]
Req. Data 1	Solar Wind Velocity at L1	Coronagraph Imagery of Sun-Earth Line	Solar Wind Velocity at 1AU Behind Earth
Lead Times	12 min	14 h	~1 dy to 27 dy
Range	250–2500km/s 1/min cadence 10 min latency (NRT)	1.4–15 Rs 4/h cadence 10 h latency (NRT)	250–800km/s 1/min cadence ~dy latency (NRT)
Req. Data 2	Solar Wind Density at L1	Heliospheric Imagery of Sun-Earth Line	Solar Wind Density at 1 AU Behind Earth
Range	0.1–150 cm^{-3} 1/min cadence 10 min latency (NRT)	15–84 Rs >1/h cadence 6 h latency (NRT)	0.1–50 cm^{-3} 1/min cadence ~dy latency (NRT)
Req. Data 3	Magnetic Field Vector at L1	Coronagraph Imagery from Sun-Earth Line	—
Range	±0.1–200 nT 1/min cadence 10 min latency (NRT)	2.4–6 Rs 5/h cadence 10 h latency (NRT)	—

[a]Extended Lead-Time Forecasting of CIR arrival time is added as the single auxiliary geomagnetic storm forecasting category that is based solely on NASA data.

2.3.4. Extended Lead-Time Forecasting Models and Data Requirements

Fast streams of CIRs emanate from coronal holes at the Sun. They can be long lived and extend down into the ecliptic plane, where they can encounter Earth and lead to geomagnetic activity. As mentioned above, a simple in situ method exists that extrapolates observations from any location trailing Earth in its orbit by assuming quasi-stationary solar wind structure and any necessary correction for radial difference [*Williams et al.*, 2011; *Vennerstrom et al.*, 2003]. This method predicts the arrival time of a CIR at Earth. *Williams et al.* [2011] show that this method is slightly better in predicting CIR arrival times than a method observing CIR structures with heliographic imagery. The data required for CIR prediction with this method are solar wind velocity in the typical range for quiet-time solar wind (250–800 km/s) and interplanetary magnetic field measurements [*e.g., Gopalswamy et al.*, 2011].

2.3.5. Preevent-Based Forecasting Models and Data Requirements

Current research addresses the challenge of space weather with attempts to improve modeling of the Sun-inner heliosphere-geospace region. Notably, there currently are no experimental models undergoing model verification and validation that are based on preevent observations with the exception of probabilistic forecasting tools. The forecasts aiming at the longest lead times currently available derive methods that attempt to forecast solar activity of which the eruptions of CMEs are one aspect. These solar activity forecasting methods utilize measures such as the free magnetic energy in the fields of active regions [*Falconer et al.*, 2011], far-side imaging of sunspots [*Lindsey and Braun*, 2000], or even the attempts of observations of upwelling of magnetic fields under the photosphere [*Reinard et al.*, 2010]. These attempts have future potential—if coupled with other simulations, tools, or models—to provide an end-to-end forecasting architecture with lead times exceeding those given by the propagation of CMEs to 1 AU. However, as the focus of this assessment is the space-based assets used as input to research to operations of transient geomagnetic storm forecasting at Earth, the above methods currently do not provide us with any specific information to be evaluated against beyond probabilities of occurrence within a period of days.

2.4. Data Requirements Summary

Table 1 summarizes the assumed data requirements for the purpose of the NRT and archival assessment. The latency requirement applies only to the NRT assessment. We find that within-range time resolutions and accuracies achieved by existing instrumentation are sufficient for making progress toward NRT warnings and archival model improvements. The significant exceptions are the parameter range for the NRT solar wind velocity, which needs to be extended considerably, and the robustness of, in particular, NRT solar wind plasma measurement with respect to solar energetic particles (SEPs).

3. SWx Assessment

Section 3.1 describes the data collected for this assessment and the single assessment criterion, reliability of observations during the historical extremes of space weather. Sections 3.2–3.5 assess the space weather reliability for short-term geomagnetic storm forecasting, for long-term geomagnetic storm forecasting, for CIR arrival time forecasting, and for preevent based forecasting.

3.1. SWx Assessment Data Collection

This study relies on solicited responses from NASA-supported teams that have built the suite of currently or near-future operating space instruments with significant space weather applicability.

The NASA Heliophysics System Observatory currently comprises 18 missions, several of which are shared with other domestic or international agencies, with a total of 29 individual spacecraft. All NASA Heliophysics research data are quality checked and made public by the operating-mission teams through openly accessible archives. In addition, six of the missions provide the Heliophysics and space weather communities with NRT data: the Advanced Composition Explorer ACE [*Stone et al.*, 1998], the Van Allen Probes (formerly known as Radiation Belt Storm Probes/RBSP) [*Mauk et al.*, 2012], the Solar and Heliospheric Observatory SOHO [*Fleck et al.*, 1995], the Solar Dynamics Observatory SDO [*Pesnell et al.*, 2012], the Solar-Terrestrial Relations Observatory STEREO [*Kaiser et al.*, 2008], and Wind [*Acuňa et al.*, 1995]. The NRT data are transmitted either through beacon downlink (ACE), the Deep-Space Network or other downlink networks (SDO, SOHO, Van Allen Probes, Wind), or a combination of the two (STEREO). Archival data also rely on these downlinks, with the exception of beacons. In the future, and under the aegis of NOAA, the Deep Space Climate Observatory (DSCOVR) is expected to be added to this list.

As part of a U.S. government interagency assessment [*Williamson et al.*, 2013], a request was sent out in late spring of 2011 to the NASA instrument providers. It was aimed at meaningfully assessing the reliability of the observational system with special emphasis on severe space weather conditions. NRT data latency and measurement cadence information were sought in order to compare with the available warning time for a given space weather effect. Furthermore, the purpose was to examine whether extreme magnitudes of environmental parameters would be measurable and thus geomagnetic responses predictable with the instrumentation in place, or whether the space environment itself would impede any of the systems in the current architecture. This current analysis is intended to determine space weather impacts on both NRT and archival data products. The quality of archival data products has not been included in the NASA request but is well documented for the existing products and therefore is discussed in this study.

The teams were asked to respond to the following issues:

1. *Near-real-time data latency and cadence* concerning generated higher-level data products. Individual near-real-time data products and their respective latencies and cadences were to be identified by the teams.
2. *Coverage of extremes.* Would the instrument/sensor cover extreme conditions encountered in the most severe events, such as brightness/intensity, particle intensity, speed, etc.? Limitations were to be quantified under extreme conditions. For a typical extreme event, for what period of time would the instrument/sensor not provide reliable near-real-time information? Are there strategies for mitigating the outages or the lack of confidence in the observations of extremes?
3. *Operational limitations*. Would there be any instrument/sensor operational limitations that reduce the availability of near-real time data, including periodic bake-outs, planned or unplanned reboots, adjustments, spacecraft maneuvers, downlink limitations, etc.? What is the impact in terms of average percentages of time that the instrument/sensor is not available? Could periodic outages of the instrument/sensor be coordinated with other related data sources (same or other spacecraft (S/C)) that could minimize the impact on space situational awareness?
4. *Other.* The teams were encouraged to identify other limiting factors relevant to this assessment.

Data so obtained were entered into an assessment table (Table 2).

The table identifies spacecraft, instrument, and subsensor. For each sensor, observational channels with potential space weather forecasting capability (one or more) have been identified. The observations are judged on four factors against the requirements intrinsic to a given phenomenon: (1) coverage, (2) latency, (3) cadence, and (4) reliability under extreme space weather conditions. The archival assessment does not

AGU Space Weather

10.1002/2013SW001007

Table 2. Summary of High-Level Performance Information and SWx Assessment Result for (Now or Soon) Operating Instruments With Space Weather Forecasting Utility[a]

Category Main Aux. S/C Instr./Sensor	Obs.	Forecasting Category/Method	NRT Cov. [%] Req. Met?	Latency [min] Req. Met?	Cad. [min] Req. Met?	Coverage Extr. Req. Met?	All Req Met for NRT? for Arch.?
SLT Main	**IMF**	***Short Lead-Time***	**yes**	**yes**	**yes**	**yes**	**yes**
All IMF	**B_Z (nT)**	***Geomagnetic Storm Forecasting***					**yes**
ACE	IMF	*Geospace modeling with L1*	97	10	1	yes	yes
MAG	B (nT)	*Input B (with Vsw, Nsw)*	yes	yes	yes		yes
Wind	IMF	*Geospace modeling with L1*	~10	~5	1.5	yes	no
MFI	B (nT)	*Input B (with Vsw, Nsw)*	no	yes	yes		yes
*DSCOVR**	IMF	*Geospace modeling with L1*	*100*	*5*	*0.17*	*yes*	*yes*
(MAG)	B (nT)	*Input B (with Vsw, Nsw)*	*yes*	*yes*	*yes*		*yes*
SLT Main	**Solar Wind**	***Short Lead-Time Geomagnetic***	**yes**	**yes**	**yes**	**no**	**no**
All SW	**V, N, T**	***Storm Forecasting***					**yn**
ACE	Solar wind	*Geospace modeling with L1*	97	10	~1	no	no
SWEPAM	V, N, T	*Input Vsw, Nsw (with B)*	yes	yes	yes		y/n
ACE	Solar wind	*Geospace modeling with L1*	0	10	12	no	no
SWICS	v, N, T	*Input Vsw, Nsw (with B)*	no	yes	no		no
SOHO	Solar wind	*Geospace modeling with L1*	~50	~5	1	no	no
CELIAS-UMTOF	V, N	*Input Vsw, Nsw (with B)*	y/n	yes	yes		no
Wind	Solar wind	*Geospace modeling with L1*	~10	~5	1.5	y/n	no
SWE	V, N, T	*Input Vsw, Nsw (with B)*	no	yes	yes		y/n
*DSCOVR**	Solar wind	*Geospace modeling with L1*	100	~5	0.17	no	no
(SWE)	V, N, T	*Input Vsw, Nsw (with B)*	yes	yes	yes		no
LLT Main	**CME 2.2–30 Rs**	***Long Lead-Time Geomagnetic***	**no**	**yes**	**yes**	**no**	**no**
All Coronagraph		***Storm Forecasting***					**no**
STEREO	CME imagery 1.4–4 Rs	*CME arr. time forec. with Sun-Earth*	20–95	~30	9	y/n	no
SECCHI/COR1		*line coronagraph obs.*	no	yes	yes		y/n
STEREO	CME imagery 2.5–15 Rs	*CME arr. time forec. with Sun-Earth*	20–95	~30	15	y/n	no
SECCHI/COR2		*line coronagraph obs.*	no	yes	yes		y/n
STEREO	CME imagery 15–84 Rs	*CME arr. time forec. with Sun-Earth*	20–95	~30	40	no	no
SECCHI/HI1		*line heliospheric imaging*	no	yes	yes		no
STEREO	CME imagery 66–318 Rs	*CME arr. time forec. with Sun-Earth*	20–95	~30	120	no	no
SECCHI/HI2		*line heliospheric imaging*	no	yes	yes		no
SOHO	CME imagery 2.2–6 Rs	*CME arr. time forec. with Sun-Earth*	~50	90	12	no	no
LASCO/C2		*line based coronagr. obs.*	y/n	yes	yes		no
SOHO	CME imagery 3.7–30 Rs	*CME arr. time forec. with Sun-Earth*	~50	90	30	no	no
LASCO/C3		*line based coronagr. obs.*	y/n	yes	yes		no

AGU Space Weather

10.1002/2013SW001007

Table 2. (continued)

Category Main/Aux. S/C Instr./Sensor	Obs.	Forecasting Category/Method	Req. NRT Cov. [%]	Req. Latency [min]	Req Cad. [min]	Req Coverage Extr	All Req Met NRT AR
LLT Aux.	**EUV Imag.**	***Long Lead-Time Geomagnetic***	**yes**	**yes**	**yes**	**y/n**	**y/n**
All EUV Sol. Imag.		***Storm Forecasting***					**y/n**
SDO	EUV imagery 17.1 nm	*CME arr. time forec. with Sun-Earth*	99	30–45	0.2	y/n	y/n
AIA		*line based EUV imaging*	yes	yes	yes		y/n
LLT Aux.	**Type-II Radio Burst Det.**	***Long Lead-Time Geomagnetic***	**no**	**yes**	**yes**	**yes**	**no**
All Coronal Shock Det.		***Storm Forecasting***					**yes**
STEREO	Solar radio Type-II RB	*CME arr. time forec. with Sun-Earth*	20–95	~30	1	yes	no
SWAVES		*line based radio Type-II Obs.*	no	yes	yes		yes
LLT Aux.	**Loss Cone Det. with Rel. Ions**	***Long Lead Time Geomagnetic***	**y/n**	**yes**	**yes**	**no**	**no**
All In Situ Magn. Cloud Det.		***Storm Forecasting***					**no**
*RBSP**	Protons 50 MeV–5 GeV	*CME approach detection with*	15–85	30	0.01 yes	no	no
PSBR/RPS		*Geospace/L1-based cosmic ray obs.*	no	yes			no
LLT Aux.	**Supra-th. Ions 10–100 keV**	***Long Lead-Time Geomagnetic***	**yes**	**yes**	**yes**	**no**	**no**
All In Situ Foreshock Det.		***Storm Forecasting***					**no**
ACE	Ions >50 keV	*CME approach detection with*	97	10	1.6	no	no
EPAM/LEMS		*foreshock ions*	yes	yes	yes		no
Wind	Ions >50 keV	*CME approach detection with*	10	~5	N/A	no	no
3DP		*foreshock ions*	no	yes	no		no
PEB Main	**Full-Disk Magnetograms**	***Pre-Event Based Forecasting***	**yes**	**yes**	**yes**	**yes**	**yes**
All Sol. Activity Forec.							**yes**
SDO	Solar full-disk magnetogram	*Solar activity forecasting with*	99	5	15	yes	yes
HMI		*helioseismic methods*	yes	yes	yes		yes
SDO	Solar full-disk magnetogram	*Solar activity forecasting with coronal*	99	5	15	yes	yes
HMI		*potential magnetic field energy models*	yes	yes	yes		yes

require NRT coverage, but it requires data continuity in the archival record. The overall score is determined by the expected (or determined) performance; i.e., Would actionable required space weather data continuously be available in NRT or after the storm under extreme space weather conditions?

3.2. SWx Assessment of Short-Term Forecasting of Geomagnetic Storms

NRT magnetic field measurements at L1 are reliably provided to researchers and forecasting centers by the ACE spacecraft's RTSW (Real Time Solar Wind) chain [*Zwickl et al.*, 1998]. The assessment found that the coverage has been performing at the 97% level. Magnetic field measurements on ACE are reliably provided by the MAG instrument [*Smith et al.*, 1998]. From the sensor point of view, extreme space weather conditions would make measurements simpler as the magnetic field magnitude usually is enhanced over the noise background as compared to quiet solar wind conditions.

Concerning the complementary solar wind measurements, ACE provides NRT data at the same basic coverage as for magnetic field data. Its solar wind sensor, the Solar Wind Electron Proton Alpha Monitor (SWEPAM) [*McComas et al.*, 1998], is sensitive to the presence of high-energy solar particles. Thus, solar wind data are reliable only for nominal background and moderate events. The majority of severe or extreme space weather events that encounter Earth do so simultaneously with the presence of large fluxes of SEPs. These frequently overwhelm the SWEPAM instrument, a situation that can last for days. Concerning this situation during the Halloween event, *Skoug et al.* [2004] explain: "Two issues affected the SWEPAM data during the October and November 2003 events. First, penetrating radiation from the intense solar energetic particle event led to high instrument background levels, which at times caused the solar wind tracking algorithm to fail. At these times (from 1241 UT on 28 October through 0051 UT on 31 October and again from 0225 to 1956 UT on 3 November), track mode data were collected at the lowest possible energies, from approximately 250–1870 eV/q, which did not cover the solar wind beam during these high-speed events. Therefore only search mode data, at energies up to 17.9 keV with 33 min time resolution, are available during these periods. … Second, for several of the highest-speed points on 29–30 October 2003, the high-energy part of the solar wind beam exceeded the search mode energy range."

The described effects are visualized in the black (NRT) and red (reconstructed) data of Figure 1.

The $>$10 MeV fluence as measured by GOES/SEM was between S2 (moderate) and S3 (strong) when NRT data from ACE were first affected. On 29 October, the radiation storm exceeded S4 (severe) levels for about 12 h. At the time of recovery, it was between S2 and S3 again. As NRT data from ACE are not always available (S2 events or above occur up to 25 times per cycle) at critical time periods, given its expected and observed performance during extreme space weather, SWEPAM is not suitable for a role as the source for this required information for NRT operations. In addition, the limited data recovery with a cadence of ~30 min limits somewhat the insights for research of extreme events with archival SWEPAM observations and their effects to be gained from archival science data. In addition, *Tóth et al.* [2007] comment on the lack of reliability of SWEPAM archival solar wind density data, an effect that was mitigated by the availability of solar wind density observations from Geotail, a spacecraft that only sporadically is in the solar wind.

Another instrument on ACE, the Solar Wind Ion Composition Spectrometer (SWICS) [*Gloeckler et al.*, 1998], also provides moments of the proton distribution function. It is currently not implemented for provision of NRT data, although this would be possible. Even if implemented, the highest cadence of the instrument, 12 min, and the latency would not allow data availability in time for NRT operational or research-to-operations utilizations but would provide low-resolution redundancy for post-event analysis.

Other assets that provide some NRT solar wind data are CELIAS [*Hovestadt et al.*, 1995] on SOHO and SWE [*Ogilvie et al.*, 1995] on Wind. CELIAS Proton Monitor (PM) solar wind readings, as shown in Figure 1 in comparison with reconstructed ACE/SWEPAM data, however, are faulty during the Halloween storm period, presumably due to a combination of effects of solar wind velocity out of the instruments' nominal range and the presence of SEPs affecting the sensor. In particular, the CELIAS Halloween storm performance shows that during the arrival of the strong shock on DOY 302 the instrument provided inaccurate or even misleading solar wind speed information. In comparison with ACE RTSW data, the faulty CELIAS data cannot be easily identified. Similar behavior is found during the arrival of the second shock on DOY 303. In both cases, an apparent upper limit of ~1000 km/s is found.

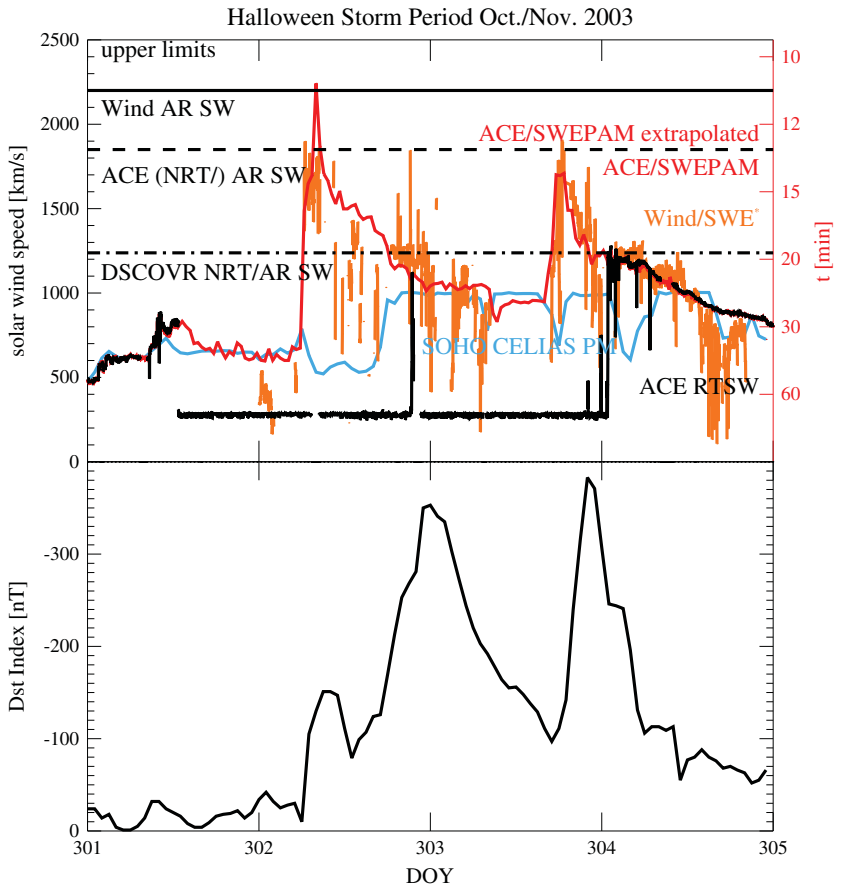

Figure 1. (top) Solar wind speeds measured at L1 (ACE, SOHO) and in the Earth's magnetotail/magnetosheath region (Wind). It includes a comparison of the ACE/RTSW solar wind real-time feed (black) with data reconstructed after the fact from ACE/SWEPAM science data by *Skoug et al.* [2004] (red) during the Halloween storms of 28 October to 1 November 2003. Data recorded by SOHO's CELIAS sensor (blue) are taken from the instrument team web site. Wind/SWE data (orange) are from *Farrugia et al.* [2005]. The horizontal lines show the upper limit of the nominal speed ranges for Wind, ACE, and DSCOVR. The approximate linear propagation time of solar wind packets of a given speed from L1 to the magnetopause is given on the right hand side. (bottom) The geomagnetic equatorial *Dst* index from the Kyoto *Dst* Index Service for comparison.

The state of health of SOHO, which in addition to CELIAS also hosts the LASCO coronagraphs and the EUV imager EIT (see further down), needs to be discussed. When it was launched in 1995, SOHO became the backbone of up to 3 day forecasts of geomagnetic storms. Foremost, the Fine and Coarse Attitude Anomaly Detection systems have failed and the spacecraft now uses monitoring of Fine Pointing Sun Sensor and Sun Acquisition Sensor for attitude anomaly detection. Without the fault detection hardware, this onboard software solution requires the central onboard computer system to be functional. As a result, certain emergency situations (one of which was experienced in the past) may no longer be survivable. In addition, SOHO has been affected by a permanent antenna motor drive malfunction. It periodically enters 2 week long so-called keyhole periods during which the downlink of continuous NRT data as required for short-term geomagnetic storm forecasting is only possible by tapping extensively into scarce 70 m DSN antenna resources. Moreover, archival data are affected by gaps. Therefore, SOHO observations do not meet the assessment criterion of continuous space weather data availability. These issues need to be considered also when we discuss long-term forecasting of geomagnetic storms, as LASCO continues to be the only source of Earth-Sun line coronagraphs, and after nearly 18 years on orbit, there are significant concerns to the health of the spacecraft.

Wind does not meet the criteria for continuous NRT availability for a combination of reasons: Deep Space Network coverage is currently limited to ~10% (2.5 h/day); although DSN coverage could be extended at the cost of science return from other NASA missions, the Wind battery performance is marginal for continuous

DSN contacts, which could be mitigated through turning off of other science instruments; the latency of Wind can be up to 10 min, which would be marginal concerning meeting the limitation of this method of 12 min, as derived from an assumed maximum solar wind speed of 2000 km/s at 1 AU, when combined with the 1.5 min delay through the cadence; current automatic NRT solar wind output has a 10% uncertainty; therefore, also the accuracy is marginal in NRT use.

Wind/SWE observations reach up to 2200km/s, i.e., 88% of the solar-wind top speed requirement of 2500km/s; therefore, its performance is judged as marginal (y/n) with respect to the archival assessment as there are historical storms that have exceeded Wind/SWE capabilities. Under normal incidence, the SWE sensor would be limited to observing up to~1238 km/s solar wind due to performance limitations in one of its components. However, Wind is a spin-stabilized S/C. This allows for the observation of higher radial solar wind velocities than for normal-incidence solar wind due to measuring the radial component of the solar wind projected on the instrument axis (~2200 km/s), almost matching the requirements of 2500 km/s. During the Halloween storms, Wind was located in the deep magnetotail/magnetosheath region behind the Earth. Figure 1 shows that the disturbed magnetosheath/solar wind plasma reaches velocities exceeding 1900 km/s, the only such occurrence since Wind was launched in 1994. Wind is now located at L1, but solar wind undisturbed from direct magnetosphere/magnetosheath influence has not exceeded ~1200 km/s (A. Szabo, personal communications, 2013). Wind and ACE currently nearly meet the archival SLT assessment requirements, but they will be 20 and 17 years old, respectively, at the time when DSCOVR will be launched.

The currently planned ACE follow-up mission for L1 is the DSCOVR. The source component of DSCOVR/SWE's performance limitations is identical with that of Wind/SWE; i.e., it will have the same limitations in normal-incidence solar wind speed. DSCOVR is a three-axis stabilized S/C. SWE is mounted such that the solar wind will enter the Faraday cup along the axis, ruling out the extension of solar wind speed range that the spin-stabilized Wind S/C utilizes. Thus, DSCOVR/SWE will not adequately cover severe or extreme space weather events beyond 1238 km/s. For comparison, the nominal limit for ACE/SWEPAM is 1850 km/s and for Wind/SWE 2200 km/s. The exact DSCOVR/SWE cutoff is yet to be verified in space. The dash-dotted line in Figure 1 shows the theoretical upper limit for reliable solar wind speed measurements for DSCOVR. Given this limitation, the future-asset DSCOVR solar wind observations fail the SWx assessment criterion for both NRT and postevent analysis.

A temporal comparison with the geomagnetic equatorial *Dst* index shows that (a) DSCOVR NRT and archival observations would fail to provide key solar wind plasma data during the most critical time, leading up to and during the geomagnetic storm main phase; (b) RTSW (NRT) observations would miss the entire shock and geomagnetic storm period. DSCOVR and ACE recover approximately at the same time; and (c) CELIAS NRT and archival observations recover between storms, but it cannot be identified from the solar wind speed whether the observations are accurate or not. (d) Wind NRT information is not available throughout any severe storm. Wind archival information will cover the entire storm period with exception of very brief periods beyond 2200 km/s. (e) ACE archival information is in low time resolution but would cover most extreme storms with the exception of brief periods above 1850 km/s. None of the current or future assets will cover in full the most extreme storms, exceeding 2200km/s, in NRT or archival information.

3.3. SWx Assessment of Long-Term Forecasting of Geomagnetic Storms

There currently are three sets of coronagraphs in service, LASCO on SOHO and the SECCHI investigation on each of the two STEREO spacecraft, A (Ahead) and B (Behind). Coronagraphs image the faint corona surrounding the Sun by blocking the light from the bright photosphere with a combination of occulter and baffles. One of the limitations encountered by coronagraphic remote sensing of solar disturbances from space is the sensitivity of the imaging (CCD) detectors to SEPs, which often occur simultaneous with CMEs. High-energy ionizing protons can directly mask the faint coronal signals in the CCDs. Depending on the fraction of the image so affected, this spurious noise can mask the otherwise observable outward speed and direction of a moving CME in consecutive images. In the worst-case scenario of fast-moving halo CMEs, it can become impossible to identify any dynamical CME parameters that depend on consecutive images of CMEs needed for speed and direction finding.

SEPs originate near the flare/CME origin and stream along open magnetic field lines into the heliosphere. It was found that there is significant particle transport across field lines to other longitudes [e.g., *Dröge*, 2003;

Lampa and Kallenrode, 2009], but the propagation time across field lines is longer than along the field. Widely distributed coronagraphs do not all get affected by early exposure to SEPs, which would allow some observations to be made during the time period of the launch of the source CME.

Furthermore, the recent 7/8 March 2012 particle events, including the most intense particle event measured near Earth since the Halloween storms, have shown that the STEREO/SECCHI/COR1 and COR2 coronagraph observations are significantly less sensitive to SEP exposure than those made by SOHO/LASCO C2 and C3. They would likely not be severely affected through even more severe events. However, extreme space weather events can cause other problems with vital S/C systems and instruments, in particular for research spacecraft that are not originally designed as space weather operational assets.

The STEREO S/C will gradually move behind the Sun and in 2014–2016 will have small angular distance from the Sun. This causes two concerns. (a) Growing distance and conjunction with the Sun reduces the data rate and causes contention with the availability of beacon ground stations, in particular converging on the period around the December solstice. The average percentage of STEREO coverage between launch and March 2013 varies by month and S/C between 20% (STEREO A, December 2012) and 95% (STEREO B, February 2009) with an overall average around 72%.

The STEREO beacons operate continuously, and the telemetry are received on the ground when stations are available. Coverage has averaged about 70%, with minima in the Northern Hemisphere winter months when the spacecraft are low in the sky. About 30% of the coverage is provided by NASA's Deep Space Network on a daily basis when the full-resolution science telemetry is downlinked. Comparable coverage is provided by an amateur radio astronomy club in Germany, and lesser amounts are captured by French and Japanese network partners. This rather limited ground station coverage leads to loss of NRT data on which the assessment result hinges. One example of NRT data loss is a coverage gap of 3 h 45 min on 11 November 2012, 0024UT–0409UT, involving STEREO A, STEREO B, and SOHO/LASCO. On this day, both STEREO S/C had 50% or more NRT coverage. There is a likely (E-limb) CME lift-off ~0220UT–0235UT visible in SDO data. STEREO beacon coverage for its coronagraphs causes particular concerns during the solar conjunction time frame. (b) The coronagraph method has seen improvements in accuracy, while the STEREO S/C were located near the quadrature positions with Earth. The improvements are a function of angular separation from Earth and of other, independent modeling improvements. As the angular separation approaches 180°, STEREO observations will merely provide redundancy for SOHO, but no significant additional angular information concerning the longitudinal/latitudinal extent of the CME. Therefore, the position-dependent (temporary) improvements of the CME arrival time forecasting will disappear. Assuming that the STEREO S/C continue to function, they will again pass through quadrature in 2019.

3.3.1. Auxiliary Method Assessment

SDO's AIA optical instrument, which allows detection of CMEs in EUV imagery, is stationed inside Earth's magnetosphere and is partially shielded from high-energy protons, which makes CME detection with this asset quite reliable. On the other hand, the imager is limited in field of view when it comes to the solar corona. Therefore, it can only observe the earliest phase of CME evolution. Direction finding and determination of the associated ICME's heliospheric full angular extent and propagation speed with AIA is still to be demonstrated through further research.

Space-based solar radio experiments are highly reliable even during extreme space weather. The signal grows with increasing CME speed. However, the method has large margins of error with respect to CME direction and speed, significantly affecting the reliability of arrival time predictions.

Detectors that sense foreshock particles with large fields of view and exposed solid-state detectors are strongly affected by the mixed radiation fields and high intensities of particles present during severe and extreme events. More robust measurements would come from detectors utilizing electrostatic deflection of ions and multiple-coincidence techniques, assuming that microchannel plate sensors can be shielded sufficiently. Although several techniques have been analyzed, the accuracy of arrival time predictions with this method is comparatively low [*Lario et al.*, 2003; *Posner et al.*, 2004], while the strength of these methods is in early detection ($>$1 h before shock arrival at the magnetopause).

3.4. SWx Assessment of CIR Arrival Time Forecasting

Arrival time prediction of CIRs currently relies on recurrence and the solar wind plasma detector PLASTIC on STEREO-B. The range of solar wind parameters of this type of space weather driver is well covered. CIRs do not

cause extreme space weather conditions at STEREO-B, but CMEs directed at STEREO-B could. The only way that STEREO-B CIR arrival time forecasting becomes impossible is when a CME arrives at STEREO-B during the time a CIR would. In this case, the arrival time method would not work, regardless of space weather conditions at the S/C.

3.5. SWx Assessment of Preevent-Based Forecasting Models

Attempts that address the forecasting of flares and CMEs [*Falconer et al.*, 2011; *Reinard et al.*, 2010, respectively] utilize observations of heliographic nature, some in connection with vector magnetograms, provided in particular by SDO's Helioseismic and Magnetic Imager (HMI). These methodologies are in the research and development phase and do not currently provide any detailed geomagnetic activity forecast information (e.g., arrival time) beyond a probability of a solar eruption within a specific time interval. It should be emphasized that this type of methodology is very robust against even the most severe types of solar storms due to the fact that the observations would be made even before the solar activity kicks in. Therefore, the analysis presented here generally does not fully apply to this sort of solar activity forecasting products, with the possible exception of data outages directly following extreme solar activity.

4. Discussion of the Overall Assessment Result and Conclusions

Effective transient geomagnetic storm forecasting should consist of a robust combination of long-term and short-term forecasting. Long-term forecasting of geomagnetic storms has the advantage of long lead times, on the order of days, that can be utilized by the end user of operational forecasts for preparations and mitigation actions. However, arrival time predictions derived solely from long-term forecasts are generally less accurate (~7.5–10 h uncertainty, presumably dependent on modeling status and STEREO location relative to Earth) as compared to short-term forecasts (~5 min). Recent improvements in CME arrival time forecasting took significant advantage of the near-ideal locations of the SOHO and STEREO coronagraphs. Currently, operational models that take advantage of coronagraph observations separated by ~180° do not exist but could be developed through further research based solely on the 2011 quadrature observations from STEREO A and B with Earth. This could help maintain our capabilities for the 2014–2016 time period. Furthermore, any NRT long-term forecast models do not incorporate the magnetic structure of magnetic clouds. These often determine the geoeffectiveness or potential damage that the disturbance may bring. Therefore, significant advances in research are still necessary in order to transfer this method to full operational use.

Coronagraph observations are currently key for feeding the leading long-term forecasting models utilized by geomagnetic storm forecasters. However, NRT coronagraph data from a single location in space can be unreliable due to sensor susceptibility to SEPs, potentially leading to situations for which long-term forecasting models for extreme storms cannot be executed. A mitigating factor is that the coronagraphs currently in use is widely spaced across the inner heliosphere; however, this is only a temporary situation. Analyses of solar particle events in the past [e.g., *Kallenrode,* 1993, and references therein] and in 2012 (exclusion of far-side flare through STEREO observations; D. McMullin, personal communication, 2012) have shown that particle transport away from the well-connected magnetic field lines occurs. This process is sufficiently slow so that the combination of widely spaced coronagraphs currently allows for sufficient coverage of severe to extreme storms. On the other hand, the STEREO S/C move farther behind the Sun and will become more limited in value to SWx forecasting as time progresses.

Gopalswamy et al. [2011] and *Webb et al.* [2010] argue that the ideal place for a future space weather mission would be at or near the L5 point of the Sun-Earth system. This would best enable the transition of research to operations for the coronagraph method. The same viewing geometry could be achieved from the perspective of L4 (see diagram at http://map.gsfc.nasa.gov/mission/observatory_l2.html). L4, however, offers one advantage over L5: the nominal magnetic field connection to the Sun of any fast central-meridian CMEs as viewed from Earth would lead SEPs away from the L4 coronagraph imager but would channel them toward the L5 imager. The nominal connection distances in longitude, given nominal background solar wind conditions, would be $>90°$ at L4, 30–70° at L1, and $<30°$ at L5. Exposure to significant fluxes of SEPs during the launch of an Earth-bound CME could lead to more than image effects for the coronagraph. A single-event upset could be more likely to disable the S/C or subsystem electronics during a most critical time if placed at L5 as compared to L4.

Short-term forecasting critically depends upon timely and accurate solar wind plasma and field observations from L1. All currently available and planned near-future L1 plasma observations fall short of the needs of NRT forecasting. With the exception of brief periods of solar wind speed exceeding 2200 km/s during the most extreme events, current missions support geospace research-to-operations needs with Wind/SWE archival data. Wind is a research S/C that will become 20 years old in 2014. A failure/loss of the S/C or the SWE instrument would not leave us with adequate archival data for this purpose. Figure 1 shows that during the only extreme event encountered in the last 20 years during which observations of the geospace response to an extreme solar wind driver were available with good quality, we are left with marginally useful solar wind observations from L1. Moreover, observations of near-future assets alone do not adequately support geospace models' research-to-operations needs or the needs for models that require archived data of severe space weather events. Most severely affected by the conditions in severe solar storms are the ACE and SOHO solar wind instruments, which in severe storms do not provide any usable NRT solar wind data due to their susceptibility to SEPs. The continuous ACE RTSW plasma data gap spans ~60 h. The NRT magnetic field data from ACE/MAG, however, are unaffected.

The solar wind monitor on SOHO also falls short due to limited availability of NRT data, driven by an antenna problem with the aging SOHO spacecraft. Wind/SWE provides some NRT solar wind plasma data, but here the S/C is susceptible to SEPs during storms that reduce accuracy of NRT data. Furthermore, lack of DSN support exists for Wind to be considered a solar wind monitor.

The situation will only partially improve with the launch of DSCOVR. DSCOVR presumably will have sufficient real-time coverage, but the Wind/SWE-derived research sensor, which cuts off at solar wind speeds between 1200 and 1250km/s, will not be capable of measuring the solar wind velocities of severe and extreme storms. During the Halloween storms, DSCOVR plasma data would not be available leading up to the two main *Dst* disturbances for a total period of 12–17 h on DOY 302 and for 5–13 h on DOY 303 (17–30 h outage time in total). Preliminary estimates from STEREO A/PLASTIC for the extreme far-side CME of 23/24 July 2012 would have led to a total outage time of 12–13 h (T. Galvin, personal communications, 2013).

Finally, the utility of L1 as a monitor location for extreme space weather events must be questioned. While there is a time of ~30 min between detection and arrival at Earth of a solar wind feature traveling at 750 km/s, this time shrinks to ~10 min or less for extreme storms. A 10 min detection time does not equal a 10 min warning time, however. The actual reaction time is reduced by processing times, validation, and, possibly the execution of a model forecasting calculation, reducing actual warning times to less than 5 min. It seems unlikely that far-reaching decisions, such as those involving dramatic protective measures applied to the power grid, will be possible based on observations with such a short lead time.

Therefore, there are no and there will not be reliable (i.e., operational) short-term warnings of severe geomagnetic storms available. Long-term, coronagraph-based warnings come with significant arrival time uncertainties, and these uncertainties will presumably grow in the 2013–2015 time frame. Current operational forecasting has to rely on magnetic field data from L1 as an indicator of an impending shock or magnetic cloud. Fortunately, during the main Halloween storm while the solar wind plasma detector was disabled, a shock compression in the magnetic field data has been observed. *Evans et al.* [2004] write that "…[a]t 0601 UTC on the 29th, a remarkably fast CME impacted the ACE spacecraft. Important sensors on ACE were already rendered useless due to the severe radiation storm; however, the transit time alone pointed to a powerful geomagnetic storm." The fact that the plasma instrument was disabled and that the determination of the shock was solely based on the magnetic field instrument has thus not been articulated clearly in the NOAA Space Environment Center (SEC) (now Space Weather Prediction Center (SWPC)) forecasting performance evaluations [*Evans et al.*, 2004].

However, this identification would not always occur. For example, quasi-parallel shock geometry would not generate any shock-signature in the magnetic field during shock passage. Even under other shock geometries, the threshold for actionable shock signatures in magnetic field data is significantly higher than that for the solar wind plasma. Therefore, significant shock event passages at L1 could be entirely missed. A forecasting system as it exists now that is based solely on robust magnetic field readings is not viable. Virtually all NRT simulations and models of the geospace system, including the critical ionosphere models that provide, e.g., ionosphere electrodynamics and auroral oval products, depend on the availability and fidelity of solar wind plasma measurements (M. Kuznetsova, personal communication, 2012). The alternative,

not available at this point due to our lack of understanding of the physics, would be a full-scale simulation of the CME as it propagates from the Sun to Earth, which could be coupled with geomagnetic modeling. Closest to this situation is the SWMF model by *Tóth et al.* [2007].

The coronagraph-based research-to-operations models (WSA-ENLIL) do not currently contain magnetic structure of ICME magnetic clouds. Therefore, these models cannot be expected to step in for the lack of solar wind plasma observations in any meaningful way to drive current geospace forecasting models. Limited solar wind data may come from sources that have less than 50% NRT coverage (SOHO/CELIAS), but the latest example of a significant storm of 7/8 March 2012 left us without any NRT solar wind data.

The importance of the current lack of the availability of reliable NRT solar wind observations during severe storms as discussed in section 3.2 and illustrated in Figure 1 cannot be stressed more. In terms of preparedness, even with near-term new assets in place, in the worst-case scenario there could be a near-complete lack of key NRT data of severe disturbances heading toward Earth. The improvement DSCOVR will bring during extreme events is solar wind plasma data continuity up to shock arrival. Even though ACE/RTSW and DSCOVR data may recover during the storm, their data will not be very useful for NRT forecasting or postevent simulations due to the fact that the state of the magnetosphere is out of equilibrium. This would cause models significant problems with the boundary conditions that would extend for quite some time beyond the solar wind plasma data gap.

In terms of research-to-operations, we know from the historical record that there will only be a few occasions per solar activity cycle during which the magnetospheric response to severe drivers can be investigated. Although Wind/SWE solar wind data can be recovered after the fact and used for archival studies, DSCOVR data cannot. The solar wind data we are left with may contain critical gaps (DSCOVR, ACE, Wind) or be in too limited resolution to be useful (ACE, see Figure 1). The lack of NRT solar wind data eliminates the option of running meaningful verification and validation of models that simulate the plentiful effects in the magnetosphere, the radiation belts, and ionosphere-thermosphere-mesosphere system [e.g., *Mays et al.*, 2009]. This includes the hampering of the development of operational products simulating GICs. Even if such a model now existed, it could not be counted on after it is transferred to operations, due to the lack of robust NRT solar wind plasma data from L1. Currently however, after-the-fact understanding of extreme geomagnetic activity could still be gained by reconstruction of the boundary conditions throughout most severe storms from Wind/SWE and ACE/SWEPAM solar wind observations with their extended range to highest speeds.

Acknowledgments

The authors gratefully acknowledge the support provided by the NASA mission and instrument teams in 2011 and helpful suggestions provided by the reviewers of the manuscript in 2012 and 2013. We also acknowledge the anonymous NOAA review provided to us in early 2013.

References

Acuña, M. H., K. W. Ogilvie, D. N. Baker, S. A. Curtis, D. H. Fairfield, and W. H. Mish (1995), The global geospace science program and its investigations, *Space Sci. Rev.*, *71*(1–4), 5–21, doi:10.1007/BF00751323.

Arge, C. N., and V. J. Pizzo (2000), Improvement in the prediction of solar wind conditions using near-real time solar magnetic field updates, *J. Geophys. Res.*, *105*(A5), 10,465–10,480, doi:10.1029/1999JA000262.

Arnoldy, R. L. (1971), Signature in the interplanetary medium for substorms, *J. Geophys. Res.*, *76*(22), 5189–5201, doi:10.1029/JA076i022p05189.

Barbieri, L. P., and R. E. Mahmot (2004), October–November 2003's space weather and operations lessons learned, *Space Weather*, *2*, S09002, doi:10.1029/2004SW000064.

Brueckner, G. E., et al. (1995), The Large Angle Spectroscopic Coronagraph (LASCO), *Sol. Phys.*, *162*(1–2), 357–402.

Carrington, R. C. (1859), Description of a singular appearance seen in the sun on September 1, 1859, Monthly Notices of the Royal Academy of Sciences, *20*, 13–15.

Claudepierre, S. G., M. K. Hudson, W. Lotko, J. G. Lyon, and R. E. Denton (2010), Solar wind driving of magnetospheric ULF waves: Field line resonances driven by dynamic pressure fluctuations, *J. Geophys. Res.*, *115*, A11202, doi:10.1029/2010JA015399.

Cliver, E. W., and L. Svalgaard (2004), The 1859 solar-terrestrial disturbance and the current limits of extreme space weather activity, *Sol. Phys.*, *224*(1–2), 407–422, doi:10.1007/s11207-005-4980-z.

Cliver, E. W., J. Feynman, and H. B. Garrett (1990), An estimate of the maximum speed of the solar wind 1938–1983, *J. Geophys. Res.*, *95*, 17,103–17,112, doi:10.1029/JA095iA10p17103.

Codrescu, M. V., C. Negrea, M. Fedrizzi, T. J. Fuller-Rowell, A. Dobin, N. Jakowsky, H. Khalsa, T. Matsuo, and N. Maruyama (2012), A real-time run of the Coupled Thermosphere Ionosphere Plasmasphere Electrodynamics (CTIPe) model, *Space Weather*, *10*, S02001, doi:10.1029/2011SW000736.

Cremades, H., O. C. StCyr, and M. L. Kaiser (2007), A tool to improve space weather forecasts: Kilometric radio emission from Wind/WAVES, *Space Weather*, *5*, S08001, doi:10.1029/2007SW000314.

Dröge, W. (2003), Solar particle transport in a dynamical quasi-linear theory, *Astrophys. J.*, *589*(2), 1027–1039, doi:10.1086/374812.

Dryer, M., Z. Smith, C. D. Fry, W. Sun, C. S. Deehr, and S.-I. Akasofu (2004), Real-time shock arrival predictions during the "Halloween 2003 epoch", *Space Weather*, *2*, S09001, doi:10.1029/2004SW000087.

Dunhak, D. W. (1979), ISEE-3, the first libration-point satellite, *Bull. Astron. Soc.*, *11*, 805.

Eccles, J. V., R. D. Hunsucker, D. Rice, and J. J. Sojka (2005), Space weather effects on midlatitude HF propagation paths: Observations and a data-driven D-region model, *Space Weather*, *3*, S01002, doi:10.1029/2004SW000094.
Evans, D. L., C. Balch, B. Murtagh, D. Zezula, L. Combs, G. Nelson, K. Tegnell, M. Crown, and B. McGehan (2004), Service assessment: Intense space weather storms October 19–November 07, 2003, U.S. Department of Commerce, National Oceanic and Atmospheric Administration, National Weather Service, Silver Spring, Md.
Falconer, D., A. F. Barghouty, I. Khazanov, and R. Moore (2011), A tool for empirical forecasting of major flares, coronal mass ejections, and solar particle events from a proxy of active-region free magnetic energy, *Space Weather*, *9*, S04003, doi:10.1029/2009SW000537.
Falkenberg, T. V., A. Taktakishvili, A. Pulkkinen, S. Vennerstrom, D. Odstrcil, D. Brain, G. Delory, and D. Mitchell (2011), Evaluating predictions of ICME arrival at Earth and Mars, *Space Weather*, *9*, S00E12, doi:10.1029/2011SW000682.
Farquhar, R. W. (1970), The control and use of libration point satellites, NASA Technical Report TR-R346.
Farrugia, C. J., et al. (2005), Interplanetary coronal mass ejection and ambient interplanetary magnetic field correlations during the Sun-Earth connection events of October–November 2003, *J. Geophys. Res.*, *110*, A09S13, doi:10.1029/2004JA010968.
Fleck, B., V. Domingo, and A. Poland (1995), The SOHO mission: An overview, *Sol. Phys.*, *162*(1–2), 1–37.
Fry, C. D., M. Dryer, Z. Smith, W. Sun, C. S. Deehr, and S.-L. Akasofu (2003), Forecasting solar wind structures and shock arrival times using an ensemble of models, *J. Geophys. Res.*, *108*(A2), 1070, doi:10.1029/2002JA009474.
Fuller-Rowell, T. J., M. C. Codrescu, and P. Wilkinson (2000), Quantitative modeling of the ionospheric response to geomagnetic activity, *Ann. Geophys.*, *18*(7), 766–781, doi:10.1007/s00585-000-0766-7.
Gao, Y., M. G. Kivelson, and R. J. Walker (2012), The linear depencence of polar cap index on its controlling factors in solar wind and magnetotail, *J. Geophys. Res.*, *117*, A05213, doi:10.1029/2011JA017229.
Gloeckler, G., et al. (1998), Investigation of the composition of solar and interstellar matter using solar wind and pickup ion measurements with SWICS and SWIMS on the ACE spacecraft, *Space Sci. Rev.*, *86*(1–4), 497–539.
Gonzalez, W. D., B. T. Tsurutani, R. P. Lepping, and R. Schwenn (2002), Interplanetary phenomena associated with very intense geomagnetic storms, *J. Atmos. Sol. Terr. Phys.*, *64*(2), 173–181, doi:10.1016/S1364-6826(01)00082-7.
Gopalswamy, N., A. Lara, S. Yashiro, M. L. Kaiser, and R. A. Howard (2001), Predicting the 1-AU arrival times of coronal mass ejections, *J. Geophys. Res.*, *106*(A12), 29,207–29,218, doi:10.1029/2001JA000177.
Gopalswamy, N., et al. (2011), Earth-Affecting Solar Causes Observatory (EASCO): A potential International Living with a Star mission from Sun-Earth L5, *J. Atmos. Sol. Terr. Phys.*, doi:10.1016/j.jastp.2011.01.013.
Horton, Q., and I. Doxas (1998), A low-dimensional dynamical model for the solar wind driven geotail-ionosphere system, *J. Geophys. Res.*, *101*(A3), 4561–4572, doi:10.1029/97JA02417.
Hovestadt, D., et al. (1995), CELIAS—Charge, element and isotope analysis system for SOHO, *Sol. Phys.*, *162*, 441–481.
Howard, R. A., D. J. Michels, N. R. Sheeley, and M. J. Koomen (1982), The observations of a coronal transient directed at Earth, *Astrophys. J.*, *263*, L101–L104, doi:10.1086/183932.
Howard, R. A., et al. (2008), Sun Earth Connection Coronal and Heliospheric Investigation (SECCHI), *Space Sci. Rev.*, *136*(1–4), 67–114, doi:10.1007/s11214-008-9341-4.
Hudson, H. S., J.-L. Bougeret, and J. Burkepile (2006), Coronal mass ejections: Overview of observations, *Space Sci. Rev.*, *123*(1–3), 13–30, doi:10.1007/s11214-006-9009-x.
Kaiser, M. L., T. A. Kucera, J. M. Davila, O. C. St. Cyr, M. Guhathakurta, and E. R. Christian (2008), The STEREO mission: An introduction, *Space Sci. Rev.*, *136*(1–4), 5–16, doi:10.1007/s11214-007-9277-0.
Kallenrode, M.-B. (1993), Neutral lines and azimuthal "transport" of solar energetic particles, *J. Geophys. Res.*, *98*(A4), 5573–5591, doi:10.1029/92JA02778.
Kappenman, J. G. (2005), An overview of the impulsive geomagnetic field disturbances and power grid impacts associated with the violent Sun-Earth connection events of 29–31 October 2003 and a comparative evaluation with other contemporary storms, *Space Weather*, *3*, S08C01, doi:10.1029/2004SW000128.
Lampa, F., and M.-B. Kallenrode (2009), Perpendicular transport in the inner heliosphere: A quick and dirty approach, *Sol. Phys.*, *260*, 423–430, doi:10.1007/s11207-009-9465-z.
Lario, D., G. C. Ho, R. B. Decker, E. C. Roelof, M. I. Desai, and C. W. Smith (2003), ACE observations of energetic particles associated with transient interplanetary shocks, in *Solar Wind Ten: Proceedings of the Tenth International Solar Wind Conference*, Pisa, Italy, 17–21 June 2002, AIP Conf. Proc., vol. 679, edited by M. Velli, R. Bruno, and F. Malara, pp. 640–643, AIP Publishing LLC, Melville, N. Y., doi:10.1063/1.1618676.
Lindsey, C., and D. C. Braun (2000), Seismic images of the far side of the Sun, *Science*, *287*(5459), 1799–1801, doi:10.1126/science.287.5459.1799.
Lopez, R. E., D. N. Baker, and J. Allen (2004), Sun unleashes Halloween storm, *EOS Trans.*, *85*(11), 105–108, doi:10.1029/2004EO110002.
Maddox, M., et al. (2010), Utilizing real-time and near real-time data in the iNtegrated Space Weather Analysis System, Abstract IN33C-08 presented at 2010 Fall Meeting, AGU, San Francisco, Calif.
Manoj, C., and S. Maus (2012), A real-time forecast service for the ionospheric equatorial zonal electric field, *Space Weather*, *10*, S09002, doi:10.1029/2012SW000825.
Mauk, B. H., N. J. Fox, S. G. Kanekal, R. L. Kessel, D. G. Sibeck, and A. Ukhorskiy (2012), Science objectives and rationale for the Radiation Belt Storm probes mission, *Space Sci. Rev.*, *179*(1–4), doi:10.1007/s11214-012-9908-y.
Mays, M. L., W. Horton, E. Spencer, and J. Kozyra (2009), Real-time predictions of geomagnetic storms and substorms: Use of the Solar Wind Magnetosphere-Ionosphere System model, *Space Weather*, *7*, S07001, doi:10.1029/2008SW000459.
McComas, D. J., S. J. Bame, P. Barker, W. C. Feldman, J. L. Phillips, P. Riley, and J. W. Griffee (1998), Solar Wind Electro Proton Alpha Monitor (SWEPAM) for the Advanced Composition Explorer, *Space Sci. Rev.*, *86*(1–4), 563–612, doi:10.1023/A:1005040232597.
Millward, G., D. Biesecker, V. Pizzo, and C. A. de Koning (2013), An operational software tool for the analysis of coronagraph images: Determining CME parameters for input into the WSA-Enlil heliospheric model, *Space Weather*, *11*, 57–68, doi:10.1002/swe.20024.
Munakata, K., J. W. Bieber, S. Yasue, C. Kato, M. Koyama, S. Akahane, K. Fujimoto, Z. Fujii, J. E. Humble, and M. L. Duldig (2000), Precursors of geomagnetic storms observed by the muon detector network, *J. Geophys. Res.*, *105*(A12), 27,457–27,468, doi:10.1029/2000JA000064.
National Research Council Workshop of the National Academies (2009), *Severe Space Weather Events—Understanding Societal and Economic Impacts: A Workshop Report*, National Academies Press, Washington, D. C.
Newell, P. T., T. Sotirelis, K. Liou, C.-J. Meng, and F. J. Rich (2007), A nearly universal solar wind-magnetosphere coupling function inferred from 10 magnetospheric state variables, *J. Geophys. Res.*, *112*, A01206, doi:10.1029/2006JA012015.
Odstrčil, D., and V. Pizzo (1999), Distortion of the interplanetary magnetic field by three-dimensional propagation of coronal mass ejections in a structured solar wind, *J. Geophys. Res.*, *104*(A12), 28,225–28,240, doi:10.1029/1999JA900319.
Odstrčil, D., P. Riley, and X. P. Zhao (2004), Numerical simulation of the 12 May 1997 interplanetary CME event, *J. Geophys. Res.*, *109*, A02116, doi:10.1029/2003JA010135.

Ogilvie, K. W., A. Durney, and T. T. von Rosenvinge (1978), Description and the experimental investigations and instruments for the ISEE spacecraft, *IEEE Trans. Geosci. Electron.*, *GE-16*(3), 151–153.
Ogilvie, K. W., et al. (1995), SWE, a comprehensive plasma instrument for the wind spacecraft, *Space Sci. Rev.*, *71*(1–4), 55–77, doi:10.1007/BF00751326.
Oler, C. (2004), Prediction performance of space weather forecast centers following the extreme events of October and November 2003, *Space Weather*, *2*, S08001, doi:10.1029/2004SW000076.
Pesnell, W. D., B. T. Thompson, and P. C. Chamberlin (2012), The Solar Dynamics Observatory (SDO), *Sol. Phys.*, *275*(1–2), 3–15, doi:10.1007/s11207-011-9841-3.
Petrukovich, A. A., S. I. Klimov, A. J. Lazarus, and R. P. Lepping (2001), Comparison of the solar wind energy input to the magnetosphere measured by Wind and Interball-1, *J. Atmos. Sol. Terr. Phys.*, *63*(15), 1643–1647, doi:10.1016/S1364-6826(01)00039-6.
Posner, A., N. A. Schwadron, D. J. McComas, E. C. Roelof, and A. B. Galvin (2004), Suprathermal ions ahead of interplanetary shocks: New observations and critical instrumentation required for future space weather monitoring, *Space Weather*, *2*, S10004, doi:10.1029/2004SW000079.
Pulkkinen, A., S. Lindahl, A. Viljanen, and R. Pirjola (2005), Geomagnetic storm of 29–31 October 2003: Geomagnetically induced currents and their relation to problems in the Swedish high-voltage power transmission system, *Space Weather*, *3,* S08C03, doi:10.1029/2004SW000123.
Pulkkinen, A., et al. (2011), Geospace Environment Modeling 2008–2009 Challenge: Ground magnetic field perturbations, *Space Weather*, *9*, S02004, doi:10.1029/2010SW000600.
Pulkkinen, A., et al. (2013), Community-wide validation of geospace model ground magnetic field perturbation predictions to support model transition to operations, *Space Weather*, *11*, 369–385, doi:10.1002/swe.20056.
Pulkkinen, T. I., M. Palmroth, H. E. J. Koskinen, T. V. Laitinen, C. C. Goodrich, V. G. Merkin, and J. G. Lyon (2010), Magnetospheric modes and solar wind energy coupling efficiency, *J. Geophys. Res.*, *115*, A03207, doi:10.1029/2009JA014737.
Rastaetter, L., M. M. Kuznetsova, A. Vapirev, A. Ridley, V. G. Merkin, A. Pulkkinen, M. Hesse, and H. J. Singer (2011), Geospace environment modeling 2008–2009 challenge: Magnetic fields at geosynchronous satellite positions, *Space Weather*, *9,* S04005, doi:10.1029/2010SW000617.
Rastaetter, L., et al. (2013), Geospace environment modeling 2008–2009 challenge: Dst index, *Space Weather*, *11*, 187–205, doi:10.1002/swe.20036.
Reinard, A. A., R. Komm, and F. Hill (2010), Predictions of active region flaring probability using subsurface helicity measurements, Abstract #SH43B-1818 presented at 2010 Fall Meeting, AGU, San Francisco, Calif.
Richardson, J. D., F. Dashevskiy, and K. I. Paularena (1998), Solar wind plasma correlations between L1 and Earth, *J. Geophys. Res.*, *103*(A7), 14,619–14,630, doi:10.1029/98JA00675.
Riley, P. (2012), On the probability of occurrence of extreme space weather events, *Space Weather*, *10*, S02012, doi:10.1029/2011SW000734.
Riley, P., J. Luhmann, A. Opitz, J. A. Linker, and Z. Mikic (2010), Interpretation of the cross-correlation function of ACE and STEREO solar wind velocities using a global MHD Model, *J. Geophys. Res.*, *115*, A11104, doi:10.1029/2010JA015717.
Schrijver, C. J., and J. P. Rabenal (2013), A survey of customers of space weather information, *Space Weather*, *11*, 529–541, doi:10.1002/swe.20092.
Simunac, K. D. C., L. M. Kistler, A. B. Galvin, M. A. Popecki, and C. J. Farrugia (2009), In situ observations from STEREO/PLASTIC: A test for L5 space weather monitors, *Ann. Geophys.*, *27*, 3805–3809, doi:10.5194/angeo-27-3805-2009.
Siscoe, G., N. U. Crooker, and C. R. Clauer (2006), Dst of the Carrington storm of 1859, *Adv. Space Res.*, *38*(2), 173–179, doi:10.1016/j/asr.2005.02.102.
Skoug, R. M., J. T. Gosling, J. T. Steinberg, D. J. McComas, C. W. Smith, N. F. Ness, Q. Hu, and L. F. Burlaga (2004), Extremely high speed solar wind: 29–30 October 2003, *J. Geophys. Res.*, *109*, A09102, doi:10.1029/2004JA010494.
Smith, C. W., J. L'Heureux, N. F. Ness, M. H. Acuna, L. F. Burlaga, and J. Scheifele (1998), The ACE magnetic fields experiment, *Space Sci. Rev.*, *86*(1–4), 613–632, doi:10.1023/A:1005092216668.
Smith, Z., and R. Zwickl (1999), Forecasting geomagnetic storms using energetic particle enhancements, in *Solar Wind Nine: Proceedings of the Ninth International Solar Wind Conference*, *Nantucket, Massachusetts, October, 1998,* vol. 471, edited by S. Habbal et al., AIP Conf. Proc., pp. 577–580, Am. Inst. of Phys., Woodbury, N. Y., doi:10.1063/1.58698.
Spencer, E. A., W. Horton, M. L. Mays, I. Doxas, and J. Kozyra (2007), Analysis of the 3–7 October 2000 and 15–24 April 2002 geomagnetic storms with an optimized nonlinear dynamical model, *J. Geophys. Res.*, *112*(A4), A04S90, doi:10.1029/2006JA012019.
St. Cyr, O. C., et al. (2000), Properties of coronal mass ejections: SOHO LASCO observations from January 1996 to June 1998, *J. Geophys. Res.*, *105*(A8), 18,169–18,186, doi:10.1029/1999JA000381.
Stone, E. C., A. M. Frandsen, R. A. Mewaldt, E. R. Christian, D. Margolies, J. F. Ormes, and F. Snow (1998), The Advanced Composition Explorer, *Space Sci. Rev.*, *86*(1–4), 1–22, doi:10.1023/A:1005082526237.
Tóth, G., D. L. De Zeeuw, T. I. Gombosi, W. B. Manchester, A. J. Ridley, I. V. Sokolov, and I. I. Roussev (2007), Sun-to-thermosphere simulation of the 28–30 October 2003 storm with the Space Weather Modeling Framework, *Space Weather*, *5*, S06003, doi:10.1029/2006SW000272.
Tsurutani, B. T., W. E. Gonzalez, A. L. C. Gonzalez, F. Tang, J. K. Arballo, and M. Okada (1995), Interplanetary origin of geomagnetic activity in the declining phase of the solar cycle, *J. Geophys. Res.*, *100*(A11), 21,717–21,734, doi:10.1029/95JA01476.
Tsurutani, B. T., W. E. Gonzalez, G. S. Lakhina, and S. Alex (2003), The extreme magnetic storm of 1–2 September 1859, *J. Geophys. Res.*, *108*(A7), doi:10.1029/2002JA009504.
Vennerstrom, S., N. Olsen, M. Purucker, M. Acuna, and J. Cain (2003), The magnetic field in the pile-up region at Mars, and its variation with the solar wind, *Geophys. Res. Lett.*, *30*(7), 1369, doi:10.1029/2003GL016883.
Webb, D. F., D. A. Biesecker, N. Gopalswamy, O. C. St. Cyr, J. M. Davila, B. J. Thompson, K. D. C. Simunac, and J. C. Johnston (2010), Using STEREO-B as an L5 Space Weather Pathfinder Mission, *Space Res. Today*, *178*, 10–16.
Weigel, R. S., A. J. Klimas, and D. Vassiliades (2003), Precursor analysis and prediction of large-amplitude relativistic electron fluxes, *Space Weather*, *1*(3), 1014, doi:10.1029/2003SW000023.
Weimer, D. R. (2005), Improved ionospheric electrodynamic models and application to calculating Joule heating rates, *J. Geophys. Res.*, *110*, A05306, doi:10.1029/2004JA010884.
Weimer, D. R., D. M. Ober, N. C. Maynard, W. J. Burke, M. R. Collier, D. J. McComas, N. F. Ness, and C. W. Smith (2002), Variable time delays in the propagation of the interplanetary magnetic field, *J. Geophys. Res.*, *107*(A8), 1210, doi:10.1029/2001JA009102.
Weimer, D. R., D. M. Ober, N. C. Maynard, M. R. Collier, D. J. McComas, N. F. Ness, C. W. Smith, and J. Watermann (2003), Predicting interplanetary magnetic field (IMF) propagation delay times using the minimum variance technique, *J. Geophys. Res.*, *108*(A1), 1026, doi:10.1029/2002JA009405.

Williams, A. O., N. J. T. Edberg, S. E. Milan, M. Lester, M. Fränz, and J. A. Davies (2011), Tracking corotating interaction regions from the Sun through to the orbit of Mars using ACE, MEX, VEX, and STEREO, *J. Geophys. Res.*, *116*, A08103, doi:10.1029/2010JA015719.

Williamson, S. P., et al. (2013), Report on space weather observing systems: Current capabilities and requirements for the next decade, Office of the Federal Coordinator for Meteorological Services and Supporting Research, Dept. of Commerce, Silver Spring, Md.

Xie, H., L. Ofman, and G. Lawrence (2004), Cone model for halo CMEs: Application to space weather forecasting, *J. Geophys. Res.*, *109*, A03109, doi:10.1029/2003JA010226.

Zheng, Y., M.-C. Fok, and G. V. Khazanov (2003), A radiation belt-ring current forecasting model, *Space Weather*, *1*(3), 1013, doi:10.1029/2003SW000007.

Zurbuchen, T. H. (2012), How likely is a space weather-induced U.S. power grid catastrophe? JASON weighs in, *Space Weather*, *10*, S08016, doi:10.1029/2012SW000844.

Zurbuchen, T. H., G. Gloeckler, F. Ipavich, J. Raines, C. W. Smith, and L. A. Fisk (2004), On the fast coronal mass ejections in October/November 2003: ACE-SWICS results, *Geophys. Res. Lett.*, *31*, L11805, doi:10.1029/2004GL019461.

Zwickl, R., et al. (1998), The NOAA Real-Time Solar-Wind (RTSW) System using ACE data, *Space Sci. Rev.*, *86*(1–4), 633–648, doi:10.1023/A:1005044300738.